



An experimental investigation of air cooling thermal module using various enhancements at low Reynolds number region

Kai-Shing Yang^a, Shu-Lin Li^b, Ing Youn Chen^b, Kuo-Hsiang Chien^c, Robert Hu^c, Chi-Chuan Wang^{a,*}

^a Department of Mechanical Engineering, National Chiao Tung University, Hsinchu 300, Taiwan

^b Mechanical Engineering Department, National Yunlin University of Science and Technology, Yunlin 640, Taiwan

^c Green Energy & Environment Research Laboratories, Industrial Technology Research Institute, Hsinchu 310, Taiwan

ARTICLE INFO

Article history:

Received 8 March 2010

Received in revised form 31 July 2010

Accepted 31 July 2010

Available online 17 September 2010

Keywords:

Heat sink

Interrupted fin

Vortex generator

Dimple

ABSTRACT

This study examines the airside performance of heat sinks having fin patterns of plate fin (Type I), interrupted fin geometry (Type II), dense vortex generator (Type III), and loose vortex generator (Type IV). Test results indicate that the heat transfer performance is strongly related to the arrangement of enhancements. The interrupted and dense vortex generator configurations normally contribute more pressure drop penalty than improvements of heat transfer. This is especially pronounced when operated at a lower frontal velocity. Actually the plain fin geometry outperforms most of the enhanced fin patterns such as of Type II and Type III at the fully developed region. This is because a close spacing prevents the formation of vortex, and the presence of interrupted surface may also suffer from the degradation by constriction of conduction path. The results suggest that the vortex generators operated at a higher frontal velocity is more beneficial than that of plain fin geometry. In association with the VG-1 criteria (same pumping power and same heat transfer capacity), the results show that effective reduction of surface area can be achieved when the frontal velocities are at 3–5 m s⁻¹ and the fin patterns are triangular, triangular attack, or two-groups dimple. The result from the present experiment suggests that the asymmetric combination such as using loose vortex generator (Type IV) can be quite effective. The triangular attack vortex generator is regarded as the optimum enhancement design for it could reduce 12–15% surface area at a frontal velocity around 3–5 m s⁻¹. The asymmetric design is still applicable even when the fin pitch is reduced to 1 mm.

© 2010 Elsevier Ltd. All rights reserved.

1. Introduction

The junction temperature significantly affects electronic components reliability, and relates exponentially to device failures [1]. The conventional air cooling featuring low heat transfer performance and noise problems is currently facing extreme difficulty to handle high flux applications, and alternatives like heat pipes, liquid immersion, jet impingement and sprays, thermoelectrics, and refrigeration are considered to be powerful solutions [2]. However, due to concerns of cost, simplicity, and reliability, air cooling is still by far the most popular thermal management of electronics, and various forms air cooled thermal module are manufactured and supplied to markets in mass quantity. Unfortunately, the considerable low thermal conductivity for air inevitably results in a very low heat transfer coefficient. The heat transfer performance of heat sink can enhance by increasing frontal velocity generally. However Li and Chao [3] indicate the enhancement of heat transfer

is limited when the Reynolds number reaches a particular value, and the noise is the major problem of operation in high frontal velocity. As a consequence, the general approach for heat transfer improvement is via exploitation smaller fin spacing to accommodate more fin surface. However, a limitation is imposed on this conventional approach when the fin spacing is small and the operation speed is low. This is because fully developed flow prevails [4]. In this sense, one would resort to interrupted fin geometry to reduce the thermal resistance. The general concept is via periodical renewal of boundary layer. Unfortunately, typical interrupted surfaces shows appreciable degradation in low velocity region pertaining to the “duct flow” phenomenon [4–6]. The results imply a dilemma situation of heat transfer augmentation occurring at a low velocity having smaller fin spacing. In essence, a difficult situation occurs for small fin spacing operated at low Reynolds number region where significant augmentation is hard to achieve.

Some alternatives to tailor above problem are to introduce swirl flow, Coanda deflection flow and destabilized flow field. The common way for this kind of implementation is using vortex generators [7] or dimple/protrusion structure [8]. Vortex generators in early research were used to delay boundary layer separation on

* Corresponding author. Address: EE474, 1001 University Road, Hsinchu 300, Taiwan.

E-mail address: ccwang@mail.nctu.edu.tw (C.-C. Wang).

Nomenclature

A	heat transfer surface area (m^2)	\dot{Q}_{conv}	convection heat transfer rate (W)
A_{ct}	cross sectional area at the test section (m^2)	Re_{dh}	duct Reynolds number (dimensionless)
A_{front}	frontal area of fins (m^2)	T_{avg}	the average temperature of the air (K)
C	perimeter of the rectangular section (m)	T_w	the average surface temperature (K)
C_f	friction factor (dimensionless)	V_c	the mean velocity in the flow channel (m s^{-1})
C_{p_a}	specific heat at constant pressure of air ($\text{J kg}^{-1} \text{K}^{-1}$)	V_{front}	the frontal velocity (m s^{-1})
D_h	hydraulic diameter (m^2)	\dot{V}	volumetric air flow rate ($\text{m}^3 \text{s}^{-1}$)
F_s	fin spacing (m)	x^+	inverse Graetz number (dimensionless)
$barh$	average convective heat transfer coefficient ($\text{W m}^{-2} \text{K}^{-1}$)	<i>Greek symbols</i>	
h_0	effective heat transfer coefficient ($\text{W m}^{-2} \text{K}^{-1}$)	ΔP	total pressure drop (Pa)
j	Colburn factor (dimensionless)	ΔT_m	effective mean temperature difference (K)
H	fin height (m)	α	aspect ratio of rectangular section (dimensionless)
H_b	thickness of base plate (m)	σ	ratio of free-flow area to frontal area (dimensionless)
L	duct length (m)	μ	dynamic viscosity (kg m s^{-1})
k	the thermal conductivity of air ($\text{W m}^{-1} \text{K}^{-1}$)	ρ	density of air (kg m^{-3})
\dot{m}	mass flow rate (kg s^{-1})	<i>Subscript</i>	
N	number of fins (dimensionless)	plate	plain fin surface
P	fin perimeter (m)		
Pr	Prandtl number (dimensionless)		

aircraft wings [9]. Recently, vortex generator is adopted for electronic cooling and the like because it reveals great potential in reducing the thermal resistance. However, the enhancements of heat transfer usually exceed pressure drop penalty. For example, Gentry and Jacobi [10] reported the average heat transfer enhancement of 20–50% with corresponding pressure drop penalty being approximately 50–110% for using vortex generators. The influence of dimple vortex generators depends on the arrangements of the dimple configuration, and the heat transfer rates and friction factors for dimpled channels are about 1.15–2.5 and 1.08–3.5 times higher than those of the smooth channel, respectively [11].

In practice, the electronic cooling applications often use very dense fin for heat-dissipation due to space limitation. Unfortunately, the dense fin arrangements lead to early fully developed flow and results in a lower heat transfer performance occurring at low Reynolds number region. In the situation, it is hard to have a significant augmentation. Though some studies had been conducted for heat transfer enhancements for electronic cooling system, the information about augmented heat transfer performance at affordable pressure drop penalty especially at lower Reynolds number region is still quite demanding. Hence the purpose of the present study is to investigate various enhancements on the overall performance pertaining to electronic cooling applications. Efforts are made toward sufficient enhancements at an affordable pressure drop penalty.

2. Experimental apparatus

The experiment apparatus is based on ASHRAE wind tunnel set-up to measure the heat transfer and the pressure drop characteristics of the heat sinks. Two main parts of the experimental apparatus are described in the following.

2.1. Wind tunnel

As seen in Fig. 1, experiments were performed in an open type wind tunnel. The ambient air flow was forced across the test section by a centrifugal fan with an inverter. To avoid and minimize the effect of flow mal-distribution in the experiments, an air straightener–equalizer and a mixer were provided. The inlet and the exit temperatures across the sample were measured by two

T-type thermocouple meshes. The inlet measuring mesh consists of four thermocouples while the outlet mesh contains eight thermocouples. The sensor locations inside the rectangular duct were established following ASHRAE [12] recommendation. These data signals were individually recorded and then averaged. During the isothermal test, the variation of these thermocouples was within 0.2 °C. In addition, all the thermocouples were pre-calibrated by a quartz thermometer having 0.01 °C precision. The accuracies of the calibrated thermocouples are of 0.1 °C. The pressure drop of the test sample and nozzle was detected by a precision differential pressure transducer, reading to 0.1 Pa. The air flow measuring station was a multiple nozzle code tester based on the ASHRAE 41.2 standard [13]. All the data signals are collected and converted by a data acquisition system (a hybrid recorder). The data acquisition system then transmitted the converted signals through Ethernet interface to the host computer for further operation.

2.2. Heat sink

A total of eight heat sinks were made and tested, the corresponding fin patterns are (a) plain fin; (b) delta vortex generators fin; (c) delta vortex generators + plain fin; (d) semi-circular vortex generators fin; (e) triangular vortex generators fin; (f) triangular attack vortex generators; (g) dimple vortex generators fin and (h) two-groups dimple vortex generators fin. The experimental results of louver and slit fin are taken from Yang et al. [4]. The delta vortex generators are of equilateral triangle. The heat sinks are made from copper with a thermal conductivity of $398 \text{ W}^{-1} \text{ m K}$. The fabricated vortex generators are punched from copper sheet, leaving holes alongside the fin. Detailed geometries of heat sink are shown in Fig. 2, and their detailed dimensions are also tabulated in Table 1. Tests are conducted at an inlet temperature of $25 \pm 2 \text{ }^\circ\text{C}$ having a relative humidity of $60 \pm 5\%$. The frontal velocity ranges from 1 to 5 m s^{-1} . The base plates of the heat sinks are of square configuration with a length/width of 50 mm and a thickness of 2 mm. The corresponding fin pitches is 1.0 mm, respectively, with a constant fin thickness of 0.2 mm. In addition, the height of the heat sinks is 10 mm. A film heater with the same size of base plate is attached to the bottom of heat sink. During the tests, electric power supply provided 25 W power input to the heater. Five temperature sensors were placed below the heat sink to measure the average

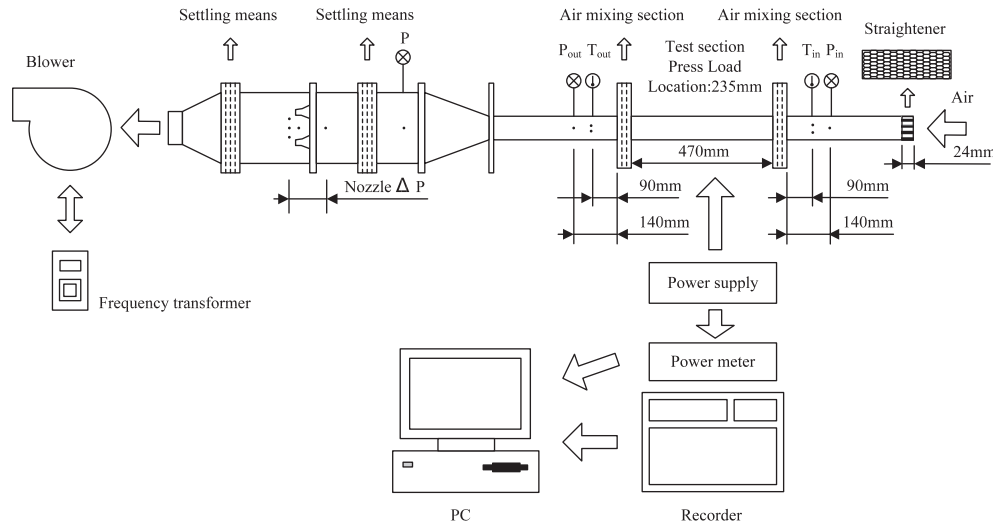


Fig. 1. Experimental set up.

Heat sink	Nomenclature	Side view	Dimension		Photos of test sample
(a) Plate	-		-	-	
(b) Delta VG			-	-	
(c) Delta VG+Plate			-	-	
(d) Semi-circular VG			-	-	
(e) Triangular VG				-	
(f) Triangular Attack VG				-	
(g) Dimple VG				-	
(h) Two Groups Dimple VG				-	

Fig. 2. All tested heat sinks in the present investigation.

temperature of the heat sink. The bakelite board is installed beneath the film heater in order to minimizing the heat loss. The heat sinks were loaded to a constant force of 11 N for all experiment. This provided consistent thermal contact resistance between the heat sinks and heater.

3. Analysis of heat sink

The airside performance of the test heat sinks are in terms of pressure drop and heat transfer performance characteristics. For determination of the friction factor of the test samples, an adiabatic test is performed to obtain the total pressure drops. Hence, the measured friction factor can be obtained from the following equation:

Table 1 Heat sink dimension. The variables are shown in Fig. 2 (Unit: mm).

L	50				
W	50				
H	10				
F_P	1				
Delta, semi-circular	Triangular	Dimple			
Opening angle	60°	S_t	2.5	D	3.05
L_{VG}	2	β	40°	d	2
W_{VG}	2	P_{t1}, P_{t2}	5, 14	δ_d	0.5
-	-	-	-	S_d	3.3
-	-	-	-	P_{d1}, P_{d2}	4, 20
-	-	-	-	δ_d/d	0.25

$$C_f = \frac{\Delta P}{4 \left(\frac{L}{D_h} \right) \cdot \left(\frac{\rho V_c^2}{2} \right)} \quad (1)$$

where L , D_h , and ρ are the duct length, hydraulic diameter and density of air. The hydraulic diameter (D_h) is defined by height of fin (H) and fin spacing (F_s), and can be obtained from the following equation:

$$D_h = \frac{4A_c}{P} = \frac{4 \times (H \times F_s)}{2 \times (H + F_s)} \quad (2)$$

The characteristic velocity is calculated by flow rate and cross sectional area at the test section as:

$$V_c = \frac{\dot{V}}{A_{ct} - A_{front}} \quad (3)$$

where \dot{V} , A_{ct} , and A_{front} represent the volumetric flow rate, cross sectional area at the test section and the frontal area of the heat sink. The total heat transfer surface area (A) is the surface in contact with work fluid, and the cross sectional area at the test section of fin (A_{ct}) is the whole flow channel of test section can be calculated as:

$$A_{ct} = W \times H \quad (4)$$

The frontal area of fins (A_{front}) can calculate by number of fins (N), thickness of fin (t) and height of fin (H) as flow:

$$A_{front} = N \times t \times H \quad (5)$$

The convective heat transfer rate of experimental system can be obtained from the following equation:

$$\dot{Q}_{conv} = \dot{m} C_p_a (T_{air,out} - T_{air,in}) \quad (6)$$

where \dot{m} , C_p_a , $T_{air,out}$ and $T_{air,in}$ represent mass flow rate, specific heat, average temperature of the inlet test section and the average temperature of the outlet test section.

The heat transfer coefficients are evaluated from the measured wall and air temperature:

$$\bar{h} = \frac{\dot{Q}_{conv}}{A_{plate} (T_w - T_{air,avg})} \quad (7)$$

where T_w is the average surface temperature and T_{avg} is the average temperature of the air at the test section. The heat transfer performance can be in terms of dimensionless Colburn j factor as

$$j = \frac{h_o}{\rho V_c C_{p_a}} Pr^{2/3} \quad (8)$$

Uncertainties in the reported experimental values were estimated by the method suggested by Moffat [14]. The highest uncertainties are 3.71% for the heat transfer coefficient and 2.02% for f . The highest uncertainties were associated with lowest Reynolds number.

4. Results and discussion

Normally the effective approach of heat transfer improvement (from $Q = hA\Delta T_m$, Q : total heat dissipated, A : area, h : convective heat transfer coefficient, ΔT_m : effective mean temperature difference) is via increase of heat dissipated area, improving convective heat transfer coefficient, or both. In this study, we have investigated various kinds of improvements characterizing the forgoing augmentations. The tested samples can be further divided into the following four categories.

Type I: Plate fin heat sink featuring heat transfer improvement from increasing heat dissipate surface. Generally, the general heat transfer augmentation is via smaller fin spacing to accommodate more fin surface.

Type II: Heat sink with interrupted fin geometry which improves convective heat transfer coefficient via periodical renewal of boundary layer and they take the form such as slit or louver fin.

Type III: Heat sink with dense vortex generator. The enhancements introduce swirl flow, Coanda deflection flow or destabilized

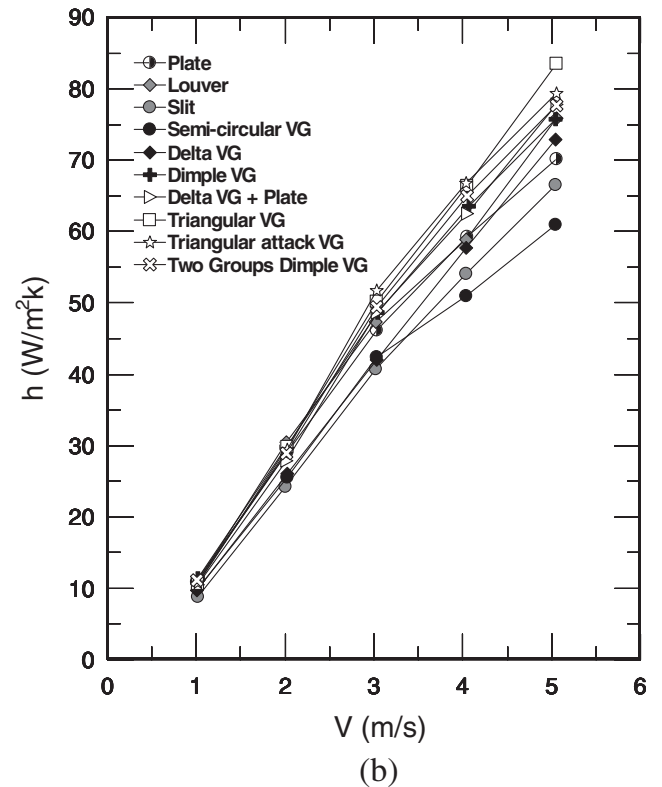
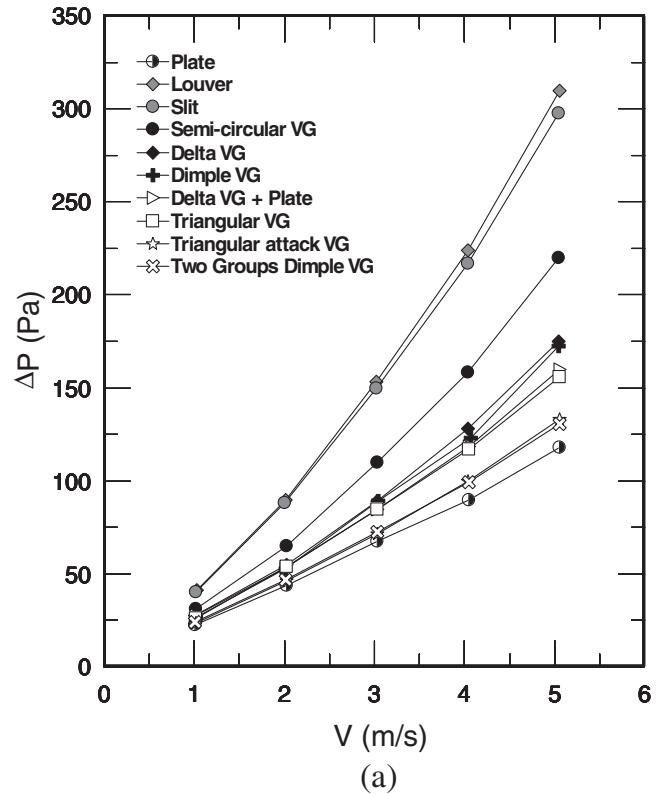


Fig. 3. (a) Pressure drops, (b) heat transfer coefficients vs. frontal velocity.

flow field from vortex generators or dimple/protrusion structure. The general arrangement is using inline or staggered layout such as semi-circular, delta and dimple vortex generator.

Type IV: Heat sink with loose vortex generator: the enhancements of this category are still vortex generators or dimple/protrusion structure but with sparse arrangement of vortex generator.

Test results of pressure drop and heat transfer coefficients vs. frontal velocity for all the test samples are plotted in Fig. 3, and dimensionless friction factor and Colburn *j* factor vs. Reynolds number are plotted in Fig. 4. As expected, pressure drop increase with the rise of frontal velocity and friction factor decrease with the rise of Reynolds number. It can be found that the friction factor for interrupted fin geometry is significantly higher than other fin types. And the louver fins show the highest friction factor among all fin pattern, followed by the dense vortex generator and loose vortex generators; the plate fin heat sink has the lowest friction factor. However, the trend of tested results on Colburn *j* factor is show that the enhancement of heat transfer does not accord with the frictional characteristics as appeared in Fig. 4. The heat transfer performance for the vortex generators exceed all other fin geometry since it can produce swirl flow, Coanda deflection flow, and destabilized flow field. Nevertheless, the arrangement of vortex generator may cast significant impact on the heat transfer performance.

At a rather low Reynolds number region, the plain fin outperforms some of the enhanced fin patterns such as semi-circular, delta VG and slit fin. The results of heat transfer performance are quite unexpected for one might expect augmentation takes control. For further explanation this unusual phenomenon, one can examine the corresponding reciprocal of the inverse Graetz number x^+ , which is defined as

$$x^+ = \frac{L/D_h}{Re_{D_h} Pr} \quad (9)$$

where *L* is the streamwise duct length and Pr is the Prandtl number. The flow may be considered fully developed when $x^+ > 0.1$ [15]. For

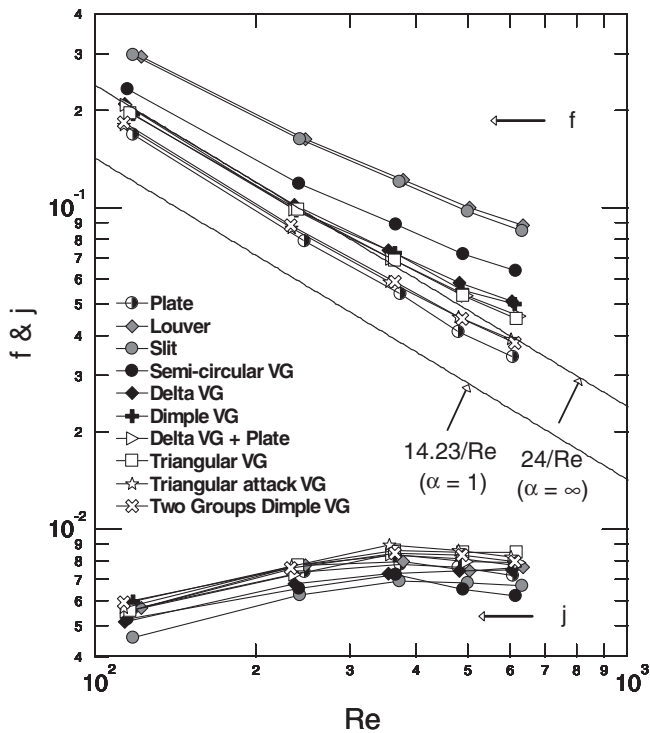


Fig. 4. Friction factor and Colburn *j* factor vs. Reynolds number for the test heat sinks.

a further comparison about the influence of developing flow on the heat transfer performance, test results are plotted in terms of variation of pressure drop penalty, $(\Delta P - \Delta P_{plate})/\Delta P$ and heat transfer augmentation, $(h - h_{plate})/h$ vs. the inverse Graetz number as depicted in Figs. 5 and 6. It is interesting to note that variation of pressure drop penalty for the surfaces can be characterized into three categories, and they are region of heat sink with interrupted fin geometry (Type II) representing the highest friction penalty relative to the plain fin geometry, region of dense vortex generator (Type III) showing moderate increase of pressure drop and region of loose vortex generator (Type IV) with only minor increase of pressure drop. In view of the results, it is generally concurred that more complicated fin structure will lead to higher pressure drop. On the other hand, the slope of variation of pressure drop penalty denotes the change of the pressure drop ratio subject to velocity variation. Apparently, the three types of fin patterns reveal completely different characteristics. The slope of Type II is nearly constant throughout test range while the slope of Type III is slightly decreased with the Reynolds number; but the slope of Type IV remains virtually unchanged as zero.

For further examination the augmentation levels shown in the figure, apparently two regions can be identified; for a lower inverse Graetz number ($x^+ < 0.1$) where the entrance effect plays a significant role, one can see substantial improvements of heat transfer through heat transfer augmentation. This is applicable to most the enhanced fin patterns being tested. Among the tested fin patterns at $x^+ < 0.1$, the heat transfer performance for heat sink with loose vortex generator (Type IV) outperforms other augmentations. On the other hand, for a fully developed situation where $x^+ > 0.1$, a clear level-off of the enhanced level for all the enhanced fin patterns is seen, and most of the augmentations of interrupted fin geometry (Type II) and dense vortex generator (Type III) fail. The

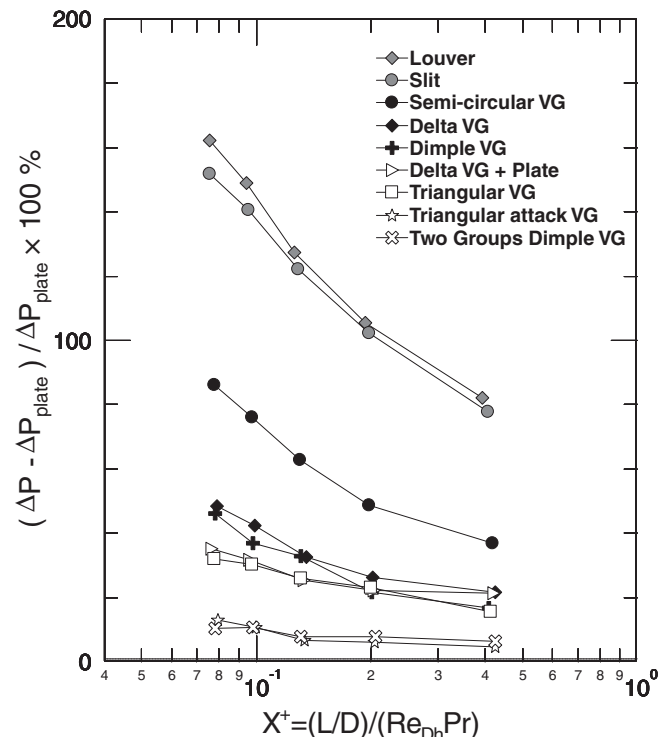


Fig. 5. Inverse Graetz number x^+ vs. pressure drop penalty for the test heat sinks.

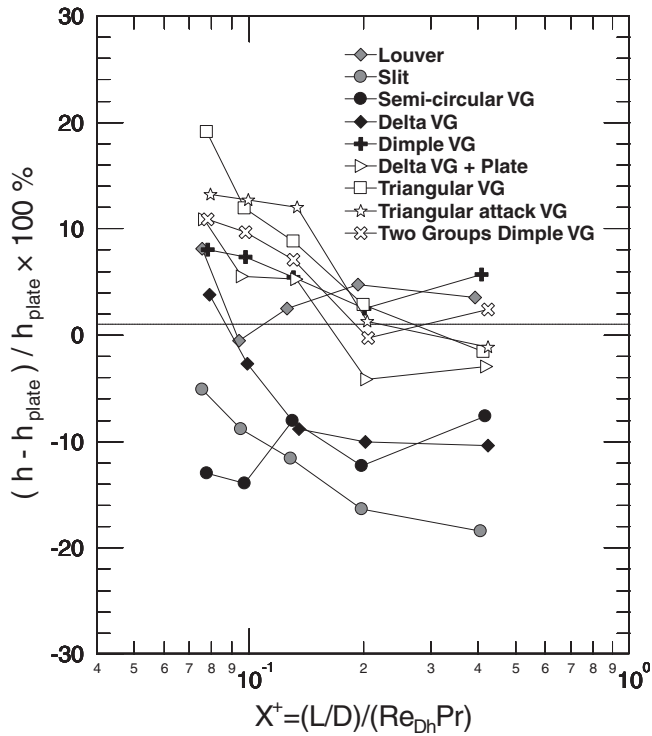


Fig. 6. Inverse Graetz number x^+ vs. variation in heat transfer coefficients for the test heat sinks.

test results suggest that the airside enhancements highly depend upon the arrangement and developing characteristics. Most of the conventional augmentation is effective only in developing regions. Yet in fully developed region, one must seek alternative enhancement using different mechanism of enhancements. The results implicate that interrupted fin and dense vortex generators fin are less effective when operated at a lower Reynolds number.

There are some explanations why most of the enhanced fin patterns fail in the fully developed region. The objective of the vortex generator is to provide swirl flow by which better mixing is achieved. However, the formation of longitudinal vortex is constrained when the fin spacing is reduced. The argument of vortex suppression can be found from a 3-D numerical investigation of a plain fin-and-tube heat exchanger performed by Torikoshi et al. [16]. Their investigation showed that the vortex forms behind the tube can be suppressed and the entire flow region can be kept steady and laminar when the fin pitch is rather small. In this sense, it explains part of the reason that the vortex generator is restrained. However, for a very low operation velocity, there is another cause for heat transfer degradation which is the blockage of conduction path of the interrupted surface. With the presence of interrupted configuration like the slit fin and semi-circular VG, the conduction path is constricted, yielding a performance drop. This phenomenon becomes more pronounced when the influence of conduction becomes more eminent. That is why at a frontal velocity of 1 m s^{-1} and a fin pitch of 1 mm, the heat transfer coefficient for plain fin exceeds most the fin patterns being tested. In fact, this effect does not occur in dimple VG fin due to continuous conduction path. In summary of the test results, the heat transfer augmentation at $x^+ > 0.1$ is very difficult via conventional interrupted surface (Yang et al. [4]) or via typical vortex generator. A more compromised design is the loose vortex generator (Type IV) design where the resistance at the downstream is lifted, giving more free space for the vortex development. As a consequence, a small enhancement of this design is seen. The test results suggest

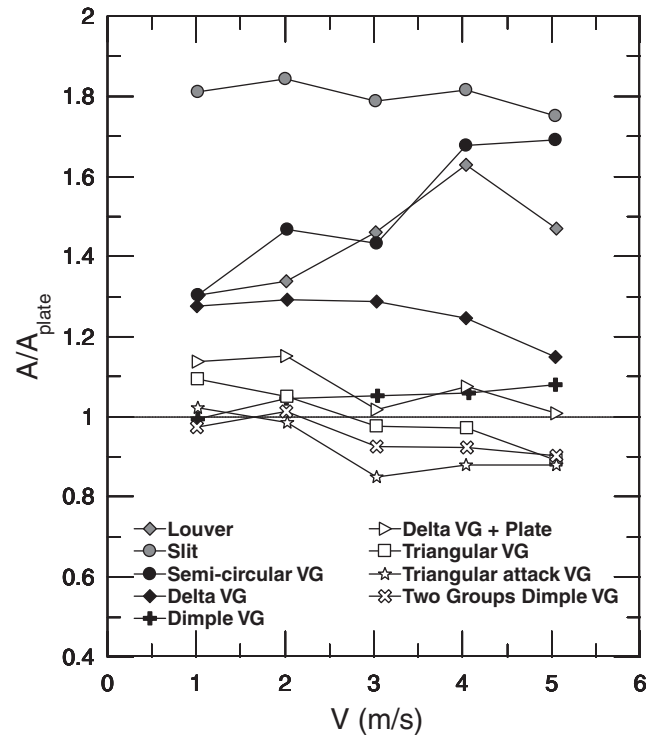


Fig. 7. Frontal velocity vs. required heat-dissipation surface area subject to VG-1 criteria.

it would be made possible from different mechanisms, e.g. unstable swing flow or asymmetric fin design.

For further performance evaluation of the tested heat sinks, comparisons are made subject to the VG-1 [17] criteria. The VG-1 criterion seeks for area reduction at the same heat transfer capacity and pumping power. As shown in Fig. 7, the ordinate of the figure is A/A_{ref} . A value above unity indicates that the required surface area for interrupted fin surface design exceeds that of plain fin surface to fulfill the same heat duty at a fixed pumping power. The results shown in this figure suggest that the vortex generators fin operated at a higher frontal velocity and arrangement of loose vortex generator is more beneficial. The results show that when frontal velocities as $3\text{--}5 \text{ m s}^{-1}$ and the fin with enhancement as triangular, triangular attack and two-groups dimple effectively reduce required surface area. The Type II and Type III fin geometry possesses the lower heat transfer coefficient in most situations along with their significant pressure drops lift them out of the choice of vortex generator subject to the VG-1 criteria. When the Reynolds number is decreased, the vortex generators would gradually surpass that of plain fin. The result from the present experiment suggests that the asymmetric combination using heat sink with loose vortex generator (Type IV) fin can be quite effective. A fin with triangular attack VG is regarded as the optimum enhancement design for it could reduce 12–15% surface area at a frontal velocity of $3\text{--}5 \text{ m s}^{-1}$. The asymmetric design is still applicable even when the fin pitch is as low as 1 mm.

5. Conclusions

The present study conducts an experimental study concerning the airside performance of heat sinks under cross flow condition. The test fin patterns can be classified into four categories, namely the base plain fin heat sink (Type I), interrupted fin geometry (Type II), dense vortex generator (Type III), loose vortex generator (Type IV) and their combinations. It is found that the heat transfer

performance is strongly related to the arrangement of enhancements. The interrupted and dense vortex generator configurations normally contribute more pressure drop penalty than improvements of heat transfer. This deterioration becomes especially evident at a lower frontal velocity. Actually the plain fin pattern outperforms most of the enhanced fin patterns of Type II and Type III at fully developed region. This is because a close spacing prohibited the formation of vortex. In the meantime, the presence of interrupted surface may also jeopardize heat conduction path due to constriction. The results indicate that the vortex generators operated at a higher frontal velocity is more beneficial than that of plain fin geometry. The results show that at a frontal velocity around $3\text{--}5\text{ m s}^{-1}$ using fins like triangular, triangular attack and two-groups dimple may be quite effective as far as surface reduction criteria is concerned. However, Type II and Type III fin geometry possesses the lower heat transfer coefficient in most situations along with their appreciable pressure drops lifts them from the choice of vortex generator subject to the VG-1 criteria. When the Reynolds number is decreased, the vortex generators would gradually surpass that of plain fin. The result from the present experiment suggests that the asymmetric combination using loose vortex generator arrangement (Type IV) can be quite effective. The triangular attack VG is regarded as the optimum enhancement design for it could reduce 12–15% surface area at a frontal velocity of $3\text{--}5\text{ m s}^{-1}$. The asymmetric design is still applicable even when the fin pitch is reduced to 1 mm.

In summary of this study, normally in the existing literatures, the heat transfer enhancements are placed in the entrance and the fully developed region. The present authors try to propose an alternative of asymmetric enhancement with the help of vortex generator instead of common interrupted surfaces. This is especially useful for air-cooling applicable for electronic devices to achieve effective augmentations without suffering from significant pressure penalty. It is therefore concluded that augmentation via various fin patterns like interrupted or vortex generator is quite effective only at developing region. However, the conventional enhanced fin patterns lose its superiority at the fully developed region. To tackle this problem, some techniques employing swing flow or unstable flow field accompanied with the asymmetric design, shows potential to resolve this problem.

Acknowledgements

The authors would like to express gratitude for supporting funding from the national science council of Taiwan (99-2218-E-009-012-MY2).

References

- [1] J.G. Maveety, H.H. Jung, Heat transfer from square pin-fin heat sinks using air impingement cooling, *IEEE Trans. Compon. Packag. Technol.* 25 (2002) 459–469.
- [2] S. Trutassanawin, E.A. Groll, S.V. Garimella, L. Cremaschi, Experimental investigation of a miniature-scale refrigeration system for electronics cooling, *IEEE Trans. Compon. Packag. Technol.* 29 (2006) 678–687.
- [3] H.Y. Li, S.M. Chao, Measurement of performance of plate-fin heat sinks with cross flow cooling, *Int. J. Heat Mass Transfer* 52 (2009) 2949–2955.
- [4] K.S. Yang, C.M. Chiang, Y.T. Lin, K.H. Chien, C.C. Wang, On the heat transfer characteristics of heat sinks: influence of fin spacing at low Reynolds number region, *Int. J. Heat Mass Transfer* 50 (2007) 2667–2674.
- [5] C.C. Wang, Extending the limit of direct air-cooling heat sink, *Heat Transfer Eng.* 29 (11) (2008) 911–912.
- [6] R.L. Webb, P. Trauger, Flow structure in the louvered fin heat exchanger geometry, *Exp. Thermal Fluid Sci.* 4 (1991) 205–217.
- [7] M. Fiebig, Embedded vortices in internal flow: heat transfer and pressure loss enhancement, *Int. J. Heat Fluid Flow* 16 (1995) 376–388.
- [8] P.M. Ligrani, G.I. Mahmood, J.L. Harrison, C.M. Clayton, D.L. Nelson, Flow structure and local Nusselt number variations in a channel with dimples and protrusions on opposite walls, *Int. J. Heat Mass Transfer* 44 (2001) 4413–4425.
- [9] G.B. Schubauer, W.G. Spangenberg, Forced mixing in boundary layers, *J. Fluid mech.* 8 (1960) 10–31.
- [10] M.C. Gentry, A.M. Jacobi, Heat transfer enhancement by delta-wing-generated tip vortices in flat-plate and developing channel flows, *J. Heat Transfer* 124 (2002) 1158–1168.
- [11] S.W. Chang, K.F. Chiang, T.L. Yang, C.C. Huang, Heat transfer and pressure drop in dimpled fin channels, *Exp. Thermal Fluid Sci.* 33 (2008) 23–40.
- [12] ASHRAE Handbook Fundamental, SI-Edition, American Society of Heating, Refrigerating and Air-conditioning Engineers, inc., Atlanta, 1993, pp. 13.14–13.15.
- [13] ASHRAE Standard 41.2-1987, Standard Methods for Laboratory Air-Flow Measurement, American Society of Heating, Refrigerating and Air-conditioning Engineers, Inc., Atlanta, 1987.
- [14] R.J. Moffat, Describing the uncertainties in experimental results, *Exp. Thermal Fluid Sci.* 1 (1988) 3–17.
- [15] J.E. Sergeant, A. Krum, *Thermal Management Handbook for Electronic Assemblies*, McGraw-Hill, New York, 1998.
- [16] K. Torikoshi, G. Xi, Y. Nakazawa, H. Asano, Flow and heat transfer performance of a plate-fin and tube heat exchanger (1st report: effect of fin pitch), 10th Int. Heat Transfer Conf., Paper 9-HE-16, 1994, pp. 411–416.
- [17] R.L. Webb, *Principles of Enhanced Heat Transfer*, John Wiley & Sons Inc., 1994.